Cobalt(II) Imino Pyridine Assisted Ethylene Polymerization: A Quantum-Mechanical/ Molecular-Mechanical Density Functional Theory Investigation

Peter Margl, Liqun Deng, and Tom Ziegler*

Department of Chemistry, The University of Calgary, 2500 University Drive NW, T2N 1N4 Calgary, Alberta, Canada

Received May 24, 1999

We investigate the new family of late-transition-metal bis(imino)pyridine (BIMP) catalysts discovered by Brookhart's (*J. Am. Chem. Soc.* **1998**, *120*, 4049) and Gibson's (*Chem. Commun.* **1998**, 849) groups by means of theoretical model calculations. Reaction pathways and energetics for chain propagation and chain termination reactions are located. Quantum-mechanical/molecular-mechanical coupling is used to expose the differences between the original [2,6-bis(1-((2,6-isopropylphenyl)imino)ethyl)pyridine]cobalt(II) catalyst and its "generic" pendant, [2,6-bis(iminomethyl)pyridine]cobalt(II). We show that the activity of the [2,6-bis(1-((2,6-diisopropylphenyl)imino)ethyl)pyridine]cobalt(II) catalyst is inhibited by steric crowding that imposes barriers on olefin capture and internal rearrangements, while at the same time increasing its activity by lowering the insertion barrier and increasing the chain termination barriers.

Downloaded by CARLI CONSORTIUM on June 30, 2009
Published on December 1, 1999 on http://pubs.acs.org | doi: 10.1021/om990392m

Introduction

Single-site olefin polymerization has recently been advanced beyond its traditional boundaries of group 4, d^0 transition-metal catalysts[1a,b] into the domain of late-transition-metal, non-d^0 catalysts by a number of groups.[1c,d] Recently, the groups of Brookhart[2] and Gibson[3] (B/G) have independently developed a set of catalysts based on the motif of the 2,6-bis(iminomethyl)-pyridine (BIMP) ligand, with various substituents on the imino nitrogen that regulate catalytic performance. This can be seen as a natural extension of previous experiments[1c,d] that were based on substituted diimine catalysts of Ni and Pd. After these recent additions, the family of non-d^0, single-site olefin polymerization catalysts involves—among others—ions of Fe, Co, Ni, and Pd. Recent studies performed in several groups—targeting the Ni and Pd systems—have exposed the skillful steric manipulation that forms the basis for the success of the Ni/Pd diimine systems:[4,5] a careful choice of steric blocking allows the formation of tailor-made polymers within a wide range of specifications for polymer molecular weight and degree of isomerization. However, the Ni and Pd diimine systems are not as active as the usual metallocene-type d^0 ones which have been studied by a number of authors.[6]

In contrast, the new Fe-based B/G catalysts exhibit astounding activity, challenging the activities of metallocenes. Their Co-based analogues are less active but were shown to produce remarkable molecular weights in some cases. It seems that, with an appropriate choice of ligands, these catalysts might pose an attractive—and above all, cheap—alternative to present-day metallocene technology.

Thus, our objective is to elucidate the mechanisms behind the catalytic performance of the Fe and Co imino pyridine systems. The present study concentrates on the Co(II) system. We shall in a large-scale density functional investigation especially target (a) the intrinsic aptitude toward polymerization of the Co(II) systems

(1) (a) Brintzinger, H. H.; Fischer, D.; Mülhaupt, R.; Rieger, B.; Waymouth, R. M. *Angew. Chem., Int. Ed. Engl.* **1995**, *34*, 1143. (b) Bochmann, M. *J. Chem. Soc., Dalton Trans.* **1996**, 255. (c) Killian, C. M.; Tempel, D. J.; Johnson, L. K.; Brookhart, M. *J. Am. Chem. Soc.* **1996**, *118*, 11664. (d) Rix, F. C.; Brookhart, M.; White, P. S. *J. Am. Chem. Soc.* **1996**, *118*, 4746.

(2) Small, B. L.; Brookhart, M.; Bennett, A. M. A. *J. Am. Chem. Soc.* **1998**, *120*, 4049.

(3) Britovsek, G. J. P.; Gibson, V. C.; Kimberley, B. S.; Maddox, P. J.; McTavish, S. J.; Solan, G. A.; White, A. J. P.; Williams, D. *J. Chem. Commun.* **1998**, 849.

(4) (a) Deng, L.; Woo, T. K.; Cavallo, L.; Margl, P. M.; Ziegler, T. *J. Am. Chem. Soc.* **1997**, *119*, 6177. (b) Deng, L.; Ziegler, T.; Woo, T. K.; Margl, P.; Fan, L. *Organometallics* **1998**, *17*, 3240. (c) Deng, L.; Margl, P.; Ziegler, T. *J. Am. Chem. Soc.*, in press.

(5) (a) Froese, R. D. J.; Musaev, D. G.; Morokuma, K. *J. Am. Chem. Soc.* **1998**, *120*, 1518. (b) Froese, R. D. J.; Musaev, D. G.; Morokuma, K. *Organometallics.* **1998**, *17*, 1850.

(6) (a) Jolly, C. A.; Marynick, D. S. *J. Am. Chem. Soc.* **1989**, *111*, 7968. (b) Castonguay, L. A.; Rappé, A. K. *J. Am. Chem. Soc.* **1992**, *114*, 5832. (c) Kawamura-Kuribayashi, H.; Koga, N.; Morokuma, K. *J. Am. Chem. Soc.* **1992**, *114*, 2359. (d) Kawamura-Kuribayashi, H.; Koga, N.; Morokuma, K. *J. Am. Chem. Soc.* **1992**, *114*, 8687. (e) Weiss, H.; Ehrig, C.; Ahlrichs, R. *J. Am. Chem. Soc.* **1994**, *116*, 4919. (f) Bierwagen, E. P.; Bercaw, J. E.; Goddard, W. A., III. *J. Am. Chem. Soc.* **1994**, *116*, 1481. (g) Woo, T. K.; Fan, L.; Ziegler, T. *Organometallics* **1994**, *13*, 2252. (h) Yoshida, T.; Koga, N.; Morokuma, K. *Organometallics* **1995**, *14*, 746. (i) Lohrenz, J. C. W.; Woo, T. K.; Ziegler, T. *J. Am. Chem. Soc.* **1995**, *117*, 12793. (j) Woo, T.; Margl, P. M.; Lohrenz, J. C. W.; Blöchl, P. E.; Ziegler, T. *J. Am. Chem. Soc.* **1996**, *118*, 13021. (k) Das, P. K.; Docker, D. W.; Fahey, D. R.; Lauffer, D. E.; Hawkins, G. D.; Li, J.; Zhu, T.; Cramer, C. J.; Truhlar, D. G.; Dapprich, S.; Froese, R. D. J.; Holthausen, M. C.; Liu, Z.; Mogi, K.; Vyboishchikov, S.; Musev, D. G.; Morokuma, K. In *Transition State Modeling for Catalysis*; ACS Symp. Ser. 721; Truhlar, D. G., Morokuma, K., Eds.; American Chemical Society: Washington, DC, 1998; pp 208−224. (l) Lanza, G.; Fragalà, I. L.; Marks, T. J. *J. Am. Chem. Soc.* **1998**, *120*, 8275.

10.1021/om990392m CCC: $18.00 © 1999 American Chemical Society
Publication on Web 12/01/1999

Chart 1

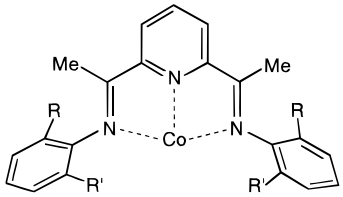

Chart 2

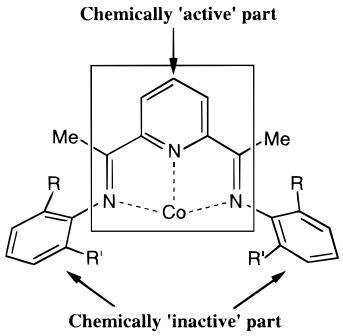

and (b) the influence of steric bulk around the active Co(II) site on catalyst performance. A detailed study of the Fe(II) system will be given elsewhere.[4c]

Computational Details

Because of the large size of the catalyst (at least 30 heavy atoms), we employ our recently developed[7a] quantum-mechanical/molecular-mechanical (QM/MM) coupling model, which is based on the IMOMM[7b] method proposed by Maseras and Morokuma (details will be described below). This allows us, essentially, to do calculations on the "real" [2,6-bis(1-((2,6-isopropylphenyl)imino)ethyl)pyridine]cobalt(II) system (system **1b**/Brookhart or **2**/Gibson, respectively) with the computational expense of a calculation on the stripped-down "model" 2,6-bis-(iminomethyl)pyridinecobalt(II). However, electronic effects such as electron flow between the bulky aryl substituents and the catalyst backbone are thus not included in our model. Previous experience with this type of approximation[4] showed, however, that this is not crucial in order to model the catalytic cycle.

The B/G cobalt catalysts (**1b** and **2** in their respective nomenclature) are shown in Chart 1. In the following, we will suppose that these catalysts are separable into a chemically "active" part, responsible for and involved in bond-making and -breaking processes, and a chemically "inactive" part, which is not involved in bond rearrangements but is thought to solely act through van der Waals forces on the active center. The active and inactive parts are outlined in Chart 2 and will be represented by different levels of theory.

Quantum-Mechanical Calculations. For the active part, where bonds are made and broken, the appropriate level of theory is a first-principles quantum-mechanical (QM) method. To describe the active part, we chose density functional theory (DFT), as it is widely regarded as the most accurate level of theory still practicable for large systems. For the majority of calculations, the ADF2.3.3 program package was used.[8] Energies and gradients for geometry optimizations were obtained self-consistently at the SVWN5+B88+P86 level of theory, which consists of the local spin-density approximation by Vosko et al. (SVWN5),[9] augmented by the gradient-corrected density functionals by Becke (B88)[10] and Perdew (P86).[11] Relativistic contributions, obtained from a first-order perturbational estimate, were added to the total energy.[12] For the transition metals, we used a triple-ζ plus polarization basis, applying the frozen-core approximation for all electrons up to and including the 2p shell. For C and N, a double-ζ plus polarization basis was used, while the 1s shell was frozen. Further methodological details on the ADF package can be found in recent publications.[13]

The SVWN5+B88+P86 (also referred to as BP86) level of theory has proven to yield results close to experiment for ethylene polymerization with homogeneous catalysts in several earlier publications. It has been shown by us that, for insertion reactions at transition-metal centers, this level of theory gives activation barriers that reproduce the experimental ones within 2−5 kcal/mol.[12] Metal−ligand bond dissociation energies are consistently overestimated by about 5 kcal/mol.[14] Recently, Jensen and Børve[15] concluded that, for olefin insertion into the Ti−C bond, BP86 yields results of comparable quality to their best level of ab initio theory, on the basis of CCSD(T) calculations.

All calculations on open-shell systems were done using a spin-unrestricted formalism. Stationary points on the potential energy surface (PES) were located by geometry optimization, until a maximum Cartesian gradient of 0.001 au was reached. Transition states were found by first doing a transit-like search whereby one selected reaction coordinate was fixed. The resultant guess for the transition state was further refined by an eigenvector-following transition state search.

Molecular-Mechanical Calculations and QM/MM Coupling. For all calculations involving the "real" system [2,6-bis(1-((2,6-isopropylphenyl)imino)ethyl)pyridine]cobalt(II), we employ a molecular-mechanics (MM) force field to model the interactions of the bulky ligands, which are predominantly steric in nature. This type of partitioning is also called quantum-mechanical/molecular-mechanical partitioning (QM/MM). The "active" part as shown in Chart 2 constitutes the *QM partition*, whereas the "inactive" part (Chart 2) constitutes the *MM partition*.

The broken N−C and C−C bonds of the QM partition are saturated with hydrogen. The Δ parameter for link bonds was set to 0.412 Å for $N-C_{methyl}$ and to 0.436 Å for the $C-C_{phenyl}$ bonds. Total energies are not particularly susceptible to these parameters. Calculations in which the parameters were interchanged showed total energies of usually within 1−2 kJ/mol of the original calculation. Torsional force field parameters crossing the phenyl link were set to zero; AMBER95 parameters[16] were used except for the vdW parameter for the metal, which was taken from UFF.[17] No electrostatic coupling of QM and MM partitions was invoked. A complete set of force field parameters is given in the Supporting Information.

Downloaded by CARLI CONSORTIUM on June 30, 2009
Published on December 1, 1999 on http://pubs.acs.org | doi: 10.1021/om990392m

(7) (a) Woo, T. K.; Cavallo, L.; Ziegler, T. *Theor. Chim. Acta* **1998**, *100*, 307. (b) Maseras, F.; Morokuma, K. *J. Comput. Chem.* **1995**, *16*, 1170.

(8) ADF 2.3.3; Theoretical Chemistry, Vrije Universiteit, Amsterdam, 1997.

(9) Vosko, S. H.; Wilk, L.; Nusair, M. *Can. J. Phys.* **1980**, *58*, 1200.

(10) Becke, A. *Phys. Rev. A* **1988**, *38*, 3098.

(11) (a) Perdew, J. P. *Phys. Rev. B* **1986**, *33*, 8822−8824. (b) Perdew, J. P. *Phys. Rev. B* **1986**, *34*, 7406.

(12) (a) Margl, P.; Ziegler, T. *Organometallics* **1996**, *15*, 5519. (b) Margl, P. M.; Ziegler, T. *J. Am. Chem. Soc.* **1996**, *118*, 7337.

(13) (a) Baerends, E. J.; Ellis, D. E.; Ros, P. *Chem. Phys.* **1973**, *2*, 41. (b) Baerends, E. J.; Ros, P. *Chem. Phys.* **1973**, *2*, 52. (c) te Velde, G.; Baerends, E. J. *J. Comput. Chem.* **1992**, *99*, 84. (d) Krijn, J.; Baerends, E. J. *Fit Functions in the HFS Method*; Department of Theoretical Chemistry, Free University: Amsterdam, The Netherlands, 1984.

(14) (a) Folga, E.; Ziegler, T. *J. Am. Chem. Soc.* **1993**, *115*, 5169. (b) Li, J.; Schreckenbach, G.; Ziegler, T. *J. Phys. Chem.* **1994**, *98*, 4838. (c) Li, J.; Schreckenbach, G.; Ziegler, T. *J. Am. Chem. Soc.* **1995**, *117*, 486. (d) Ziegler, T.; Li, J. *Can. J. Chem.* **1994**, *72*, 783. (e) Ziegler, T.; Li, J.; Schreckenbach, G. *Inorg. Chem.* **1995**, *34*, 3245.

(15) Jensen, V.; Børve, K. *J. Comput. Chem.* **1998**, *19*, 947.

(16) Cornell, W. D.; Cieplak, P.; Bayly, C. I.; Gould, I. R.; Ferguson, D. M.; Spellmeyer, D. C.; Fox, T.; Caldwell, J. W.; Kollman, P. A. *J. Am. Chem. Soc.* **1995**, *117*, 5179.

(17) Rappe, A. K.; Casewit, C. J.; Colwell, K. S.; Goddard, W. A. I.; Skiff, W. M. *J. Am. Chem. Soc.* **1992**, *114*, 10024.

Scheme 1

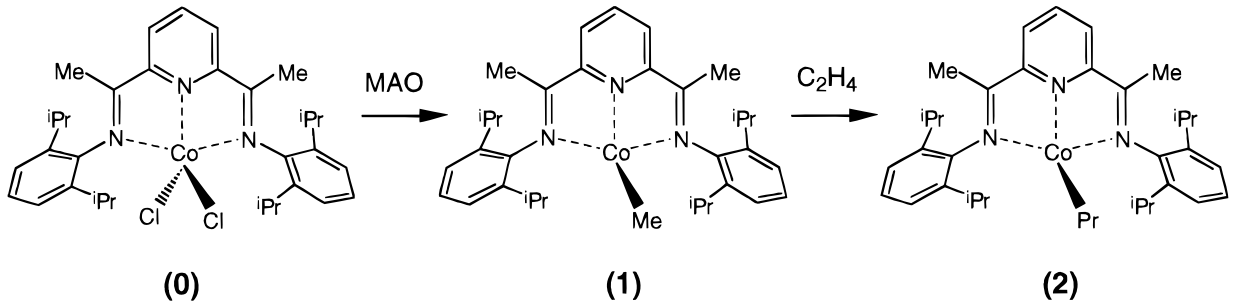

Scheme 2

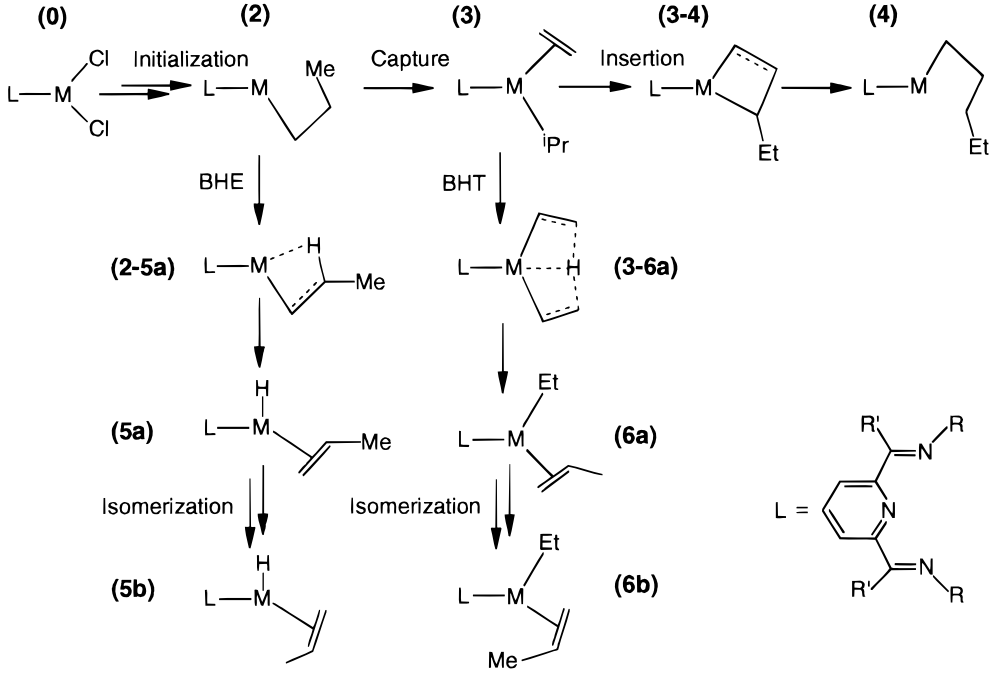

Downloaded by CARLI CONSORTIUM on June 30, 2009
Published on December 1, 1999 on http://pubs.acs.org | doi: 10.1021/om990392m

Basic Assumptions about the Catalytic Cycle. On the basis of the original papers by Brookhart's and Gibson's groups, we assumed the catalyst precursor **0** of Scheme 1 to be the metal dihalide, which, upon activation with MAO, forms the cationic species **1** of Scheme 1 with one vacant coordination site. It is furthermore assumed that **1** easily captures and inserts a monomer unit, leading to a cationic propyl species **2**, (Scheme 1). These elementary reaction events are assumed to take place only once during a catalytic run, and their kinetics are therefore not investigated here any further. *The propyl chain of* ***2*** *will in the following be regarded as a suitable model for the growing polymer chain, and* ***2*** *will henceforth be referred to as the "precursor".* The use of a propyl group as a model for the growing chain is based on previous experience with other catalysts of this type and serves to minimize the computational effort while retaining a physically accurate picture of all reactions. For instance, it has been shown that an ethyl group is not a valid model for the growing chain for some processes, most notably β-hydrogen elimination.[18,19] However, previous experience also dictates that it does not improve the accuracy of the calculations to use a chain that is longer than a propyl group.[18,19] A propyl group therefore seems the optimal choice to model the growing chain.

From this stage onward, chain propagation is believed to proceed by repeated monomer capture (**2** → **3**) and insertion into the alkyl chain (**3** → **4**), whereas chain termination events may take place either via β-hydrogen transfer to the monomer (**3** → **6**; BHT) or via β-hydrogen elimination (**2** → **5**; BHE) (Scheme 2). Alternatively, the counterion might terminate the chain via transmetalation. In the present paper, we will not investigate the influence of the counterion but instead focus on the electronic and steric factors given by the catalyst itself. Scheme 2 shows the usually accepted reaction scheme for single-site olefin polymerization. The next sections will be devoted to describing in detail the available pathways for these reactions and their energetics. Finally, on the basis of our calculations, we assume that all species except **0** have a low-spin, doublet electronic ground state. See the further discussion in the Supporting Information.

Results and Discussion

A. "Model" Systems Based on [2,6-Bis(iminomethyl)pyridine]cobalt(II). Before we turn to the "real" systems investigated by Brookhart's and Gibson's groups, we shall expose some of the intrinsic qualities of these catalysts by stripping the phenyl and methyl substituents on the ancillary ligand, capping the truncated valences with hydrogen atoms. The behavior of the resulting "model" system [2,6-bis(iminomethyl)pyridine]cobalt(II) (Chart 3) is now electronically instead of sterically dominated and allows us to separate electronic from steric influences. Table 1 shows the

(18) Margl, P.; Deng, L.; Ziegler, T. *Organometallics* **1998**, *17*, 933.
(19) (a) Margl, P.; Deng, L.; Ziegler, T. *J. Am. Chem. Soc.* **1998**, *120*, 5517−5525. (b) Margl, P.; Deng, L.; Ziegler, T. *J. Am. Chem. Soc.* **1999**, *121*, 154.

Chart 3

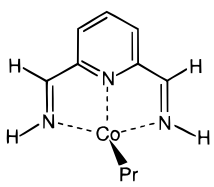

2a'

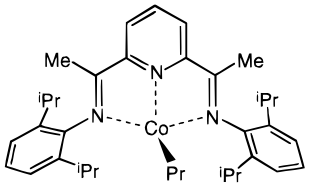

2a

Table 1. Energetics for the "Model" Catalyst[a]

category	remarks	species	energy	barrier
alkyl precursor	β-agostic	**2a′**	0	
	planar	**2b′**	12	
π-complex	β−agostic	**3a′**	−50	
	nonagostic	**3b′**	−59	
	BS	**3c′**	−63	
	apical	**3d′**	−67	
conversion TS		**3a′** → **3b′**	−45	5
		3b′ → **3d′**	−47	12
insertion TS	FS	**3b′** → **4′**	−27	32
	BS	**3c′** → **4′**	−11	52
BHT	TS	**3a′** → **6′**	−12	38
	kinetic product	**6′**	−66	
BHE	TS	**2b′** → **5′**	28	16
	kinetic product	**5′**	16	

[a] Energies in kJ/mol, relative to **2a′**. Barriers given with respect to the direct precursor of the reaction.

energy profile for the reactions outlined in Scheme 2. Note that all compounds with the 2,6-bis(iminomethyl)-pyridine ligand will be marked with primes (e.g., **2a′** of Chart 3) as opposed to those with the 2,6-bis(1-((2,6-isopropylphenyl)imino)ethyl)pyridine ligand, which will be unprimed (e.g., **2a** of Chart 3).

In previous investigations, a wide variety of possible conformations has been found for coordinatively unsaturated [L]M(alkyl) compounds such as **2′** and **3′**. For the present Co compound, we again find that there is high coordinative variability, as expressed by two distinct alkyl precursor conformations and four distinct conformations for the olefin π-complex. Formation of the π-complex proceeds in a barrierless fashion and is only moderately exothermic due to the presence of seven electrons in the d shell, which prohibit effective donation of olefin π-electrons into the metal d orbitals. The different π-complex conformations are relatively closely spaced in terms of total energy and interconvert quite easily (Table 1; **3a′** → **3b′**; **3b′** → **3d′**). We also note that FS insertion seems to be quite feasible for the "model" catalyst, with a direct barrier of 32 kJ/mol. BHT chain termination is less favorable in kinetic terms, with a direct barrier of 38 kJ/mol and a barrier relative to the most stable π-complex **3b′** of 47 kJ/mol. We also note that BHE is quite feasible for this particular catalyst, with a barrier relative to **2a′** of 28 kJ/mol. Thus, at low monomer concentration, BHE seems to compete with BHT quite effectively. We thus see that under high monomer concentration, where BHE is kinetically disfavored compared to all steps that originate from a π-complex species, the "model" catalyst [2,6-bis(iminomethyl)pyridine]cobalt(II) should be rather active and should produce a low-molecular-weight polymer. Its propagation barrier (relative to the lowest π-complex **3d′**) is 40 kJ/mol; the termination barrier (under high monomer pressure) is substantially higher (50 kJ/mol). These are values that are in the range expected for some d^0 systems.

B. The 'Real' Systems: [2,6-Bis(1-((2,6-isopropylphenyl)imino)ethyl)pyridine]cobalt. Let us now proceed to the investigation of the steric modifications imposed on the catalyst by the substituents on the ancillary ligands. Table 2 and Figure 1 list the energetics for insertion and termination pathways for the "real" system. Visual examination of Figure 1 and comparison with Table 1 reveal that the potential energy surface of the "real" system is substantially more complex than that of the "model" system (Table 1). Using the PES information given in Figure 1 as a guideline, we will now in detail examine the most probable pathways for chain propagation, termination, and possible chain isomerization.

Propagation Cycle. Chain propagation is initialized by capture of one monomer unit by the alkyl precursor species **2** to form the π-complex **3**. Among the four alkyl precursors of Chart 4, **2a** and **2b** are kinetically and thermodynamically the most stable. On the other hand, **2c** and **2d** are only marginally stable. The conversion between **2a** and **2b** (Chart 4) proceeds over a saddle point with an activation energy of 41 kJ/mol. Since there are a number of alkyl precursors, the number of capture pathways is correspondingly large. We will here consider only capture pathways that originate from **2a** or **2b**.

A visual inspection of **2a** and **2b** reveals that there are three possible pathways for olefin capture, which we have outlined in Chart 5 and classified as "Head-On", "Backside", and "Topside", respectively. From the capture energetics in Table 2 and Figure 1 it appears that none of the capture pathways are barrierless on the potential energy surface. The head-on capture pathway is sterically completely blocked, so that we were unable to locate a physically reasonable line of approach along this path. The rather substantial barriers of olefin capture are a direct effect of the heavy steric congestion around the metal center. Although the BS approach to **2b** itself is barrierless, the formation of **2b** from **2a** leads over a saddle that is 41 kJ/mol above **2a**. *Therefore, we must conclude that olefin capture to form an olefin π complex has, in contrast to the "model" system, a significant barrier on the PES.*

All uptake paths we could locate either led to **3b** or **3c**. Species **3b** (Chart 4) is the direct precursor for FS olefin insertion, whereas **3c** is the direct precursor for olefin insertion along the BS channel. However, there is a total of four interconverting π-complexes. Note that the barriers for conversions between different π-complexes are not negligible (Figure 1). The π-complex minima are quite pronounced and separated from each other by substantial barriers. This is quite in contrast with the conformational equilibrium for d^0 catalysts and also with the available data on d^8 Ni and Pd catalysts. Also, the conversion barriers are much higher than for the "model" system, suggesting that this is largely an effect of the steric bulk attached to the ancillary ligand.

The energy gained by capturing an olefin monomer strongly depends on the product conformation (Table 2). It is quite obvious from our data that olefin capture is far less exothermic than for the "model" system, in

Downloaded by CARLI CONSORTIUM on June 30, 2009
Published on December 1, 1999 on http://pubs.acs.org | doi: 10.1021/om990392m

Table 2. Energetics for the "Real" Catalyst[a]

category	remarks	species	energy	barrier
alkyl precursor	agostic	**2a**	0	
	planar	**2b**	28	
	nonagostic	**2c**	37	
	rearfacing	**2d**	36	
conversion TS		**2a → 2b**	41	41
capture TS	topside	**2a → 3b**	29	29
	backside	**2a → 3c**	25	25
	backside approach to planar precursor	**2b → 3c**		0
π-complex	FS agostic	**3a**	17	
	FS nonagostic	**3b**	−39	
	BS	**3c**	−14	
	apical	**3d**	−41	
conversion TS		**3b → 3c**	−5	34
	by opening Co−C−C angle	**3a → 3b**	28	11
		3c → 3d	40	54
	by rotating the Co−C−C−C torsion	**3a → 3b**	34	17
		3d → 3b	40	81
insertion TS	BS	**3c → 4b**	25	39
	FS	**3b → 4a**	−15	24
	apical	**3d → 4a**	27	68
pentyl insertion product	γ-agostic	**4a**	−103	
	δ-agostic	**4b**	−101	
	β-agostic	**4c**	−117	
conversion TS		**4b → 4a**	−66	35
		4a → 4c	−75	28
olefin capture TS	BS approach to γ-agostic pentyl	**4a → 9**	87 ± 5	16
BHE TS		**2b → 5a**	52	28
kinetic BHE product	hydride	**5a**	44	
BHE product	after chain ejection	**8**	183	139
BHT TS		**3a → 6a**	35	18
kinetic BHT product	ethyl+vinyl term. chain	**6a**	14	
BHT chain ejection TS		**6a → 7**	46	32
BHT product	after chain ejection	**7**	−3	
isomerization TS	after BHT	**6a → 6b**	57	43
	after BHE	**5a → 5b**	95	51

[a] Energies in kJ/mol, relative to **2a**. Barriers given with respect to the direct precursor of the reaction. Error bars relate to errors caused by insufficient geometry optimization and do not reflect errors inherent in the DFT QM/MM method or due to insufficient model assumptions.

Downloaded by CARLI CONSORTIUM on June 30, 2009
Published on December 1, 1999 on http://pubs.acs.org | doi: 10.1021/om990392m

agreement with previous studies on d^0 systems that found that the capture energy gain decreases with increasing steric bulk of the ancillary ligand. A side effect of this is that the olefin capture process is almost neutral in terms of standard free energy. We know from previous experimental and theoretical studies[19a] that the entropic contribution to the standard free energy of olefin capture is around 40−50 kJ/mol, which is exactly enough to compensate for the energy gained by π-complexation.

Monomer insertion most likely originates from **3b**, from which the lowest-lying insertion transition state **3b → 4a** can be reached with an activation energy of only 24 kJ/mol. This small activation energy—taken by itself—would give rise to an insertion rate that is comparable to the typical insertion rate for most d^0 olefin polymerization systems. Whereas FS insertion through this path is obviously quite facile, the BS insertion originating from **3c** is substantially slower, with a saddle point that lies 25 kJ/mol above the dissociation asymptote for alkyl precursor and olefin.

We have located a third, but in our opinion quite unfeasible, reaction channel that leads from the apical π-complex **3d** to **4a**. This path, however, has an activation energy of 68 kJ/mol and is thus much less attractive than the path leading over **3b → 4a**. Once it is formed from **3b**, it can neither convert back easily (80 kJ/mol activation barrier for **3d → 3b**) nor insert easily (activation barrier for **3d → 4a** 68 kJ/mol). This fact actually leads us to conclude that **3d** would act as a shallow thermodynamic sink for the propagation cycle, were it not for the rather small binding energy that allows dissociation (**3d → 2a** + olefin).

Once insertion is completed, the kinetic product of insertion can rearrange to a more stable, thermodynamic insertion product. In the present case, the two kinetic insertion products are either γ-agostic **4a** or δ-agostic **4b**. For the rearrangement cascade δ-agostic → γ-agostic → β-agostic we find barriers of 35 and 28 kJ/mol, for the first and second steps, respectively. The thermodynamic stability of the insertion product increases with decreasing order of the agostic bond (δ-agostic **4b**, −101 kJ/mol; γ-agostic **4a**, −103 kJ/mol; β-agostic **4c**, −117 kJ/mol), in agreement with findings from previous studies on d^0 systems. Again, the rather high rearrangement barriers are indicative of steric crowding in this system, since such high rearrangement barriers have never before been found for a single-site ethylene polymerization catalyst. Here, the steric pressure gives additional stability to the (compact) ground-state geometries and destabilizes the (extensive) transition-state geometries for rearrangements.

Thus, it is conceivable that an olefin molecule would much rather find the kinetic insertion product than the

Downloaded by CARLI CONSORTIUM on June 30, 2009
Published on December 1, 1999 on http://pubs.acs.org | doi: 10.1021/om990392m

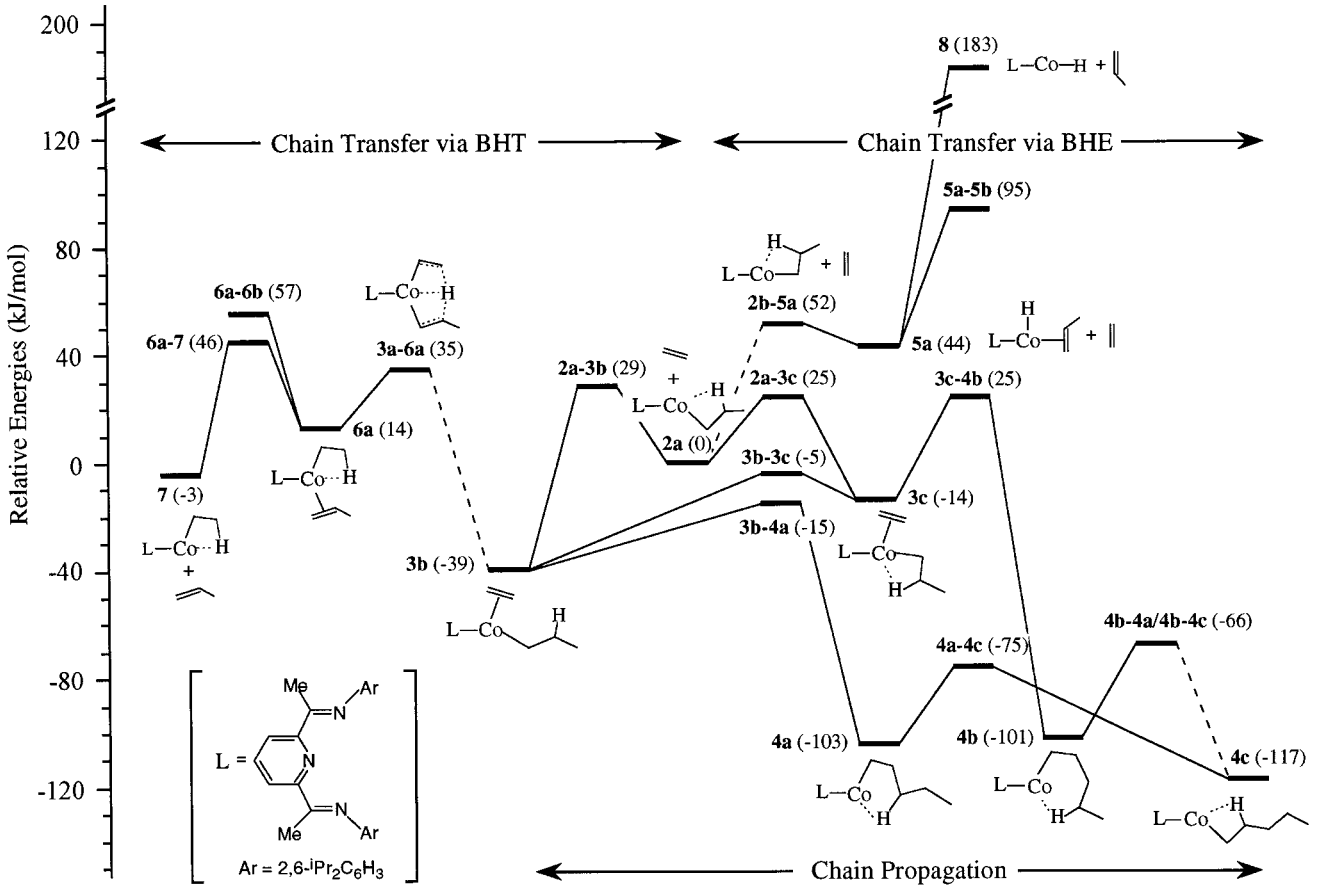

Figure 1. The most feasible reaction paths for the chain propagation, chain termination (transfer), and chain isomerization of the "real" Brookhart/Gibson cobalt(II) catalytic system. The L−Co (L = bis(imino)pyridine) coordination plane is perpendicular to the paper. A solid line represents a direct path that links the connected species. A dashed line represents an indirect path (i.e., a path exists but occurs through intermediates that are not listed).

Chart 4

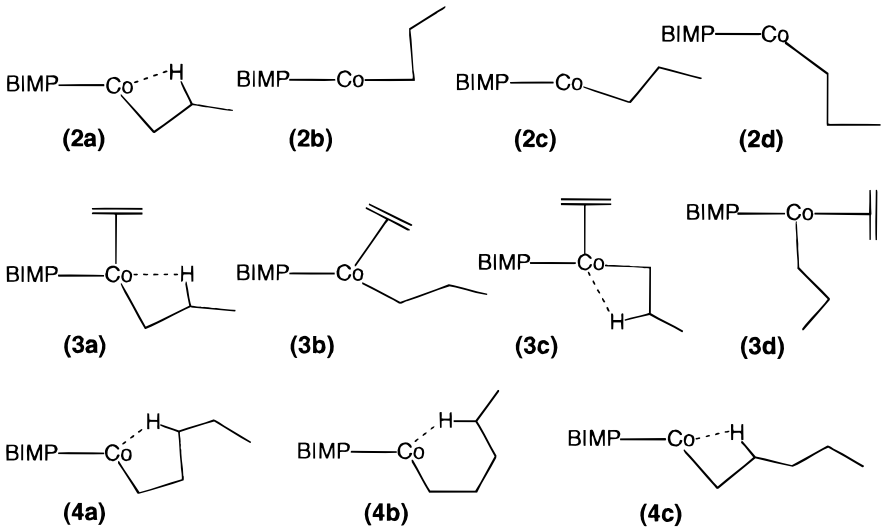

thermodynamic insertion product as it approaches the active site, since the rearrangement of the product is actually slower than the actual insertion step itself. This, in turn, means that the observed capture barrier equals the barrier **4a** → **9**, which has been located by us to be 16 kJ/mol above the energy of separated **4a** + ethylene. This corresponds to a lowering of the capture barrier as compared to capture paths that target the β-agostic alkyl precursor (**2a** → **3b**; **2a** → **3c**) by 10 kJ/mol, or an approximately 50-fold capture rate enhancement.

Having now all parts of the propagation cycle in hand, we give in Figure 1 a final picture of the propagation process as obtained by BP86 density functional theory. On the basis of our data, we project the FS propagation and the BS-FS (whereby the capture occurs in a BS

Chart 5

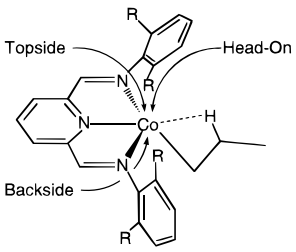

fashion, but the insertion proceeds through the FS TS) propagation pathway as two equally feasible alternatives. Within the accuracy and reliability of the applied methodology, we cannot rank these two alternatives further. The BS insertion pathway, however, seems much less attractive, since it has the relatively high-lying transition state **3c** → **4b**.

Chain Termination by BHT. In previous investigations on single-site olefin polymerization catalysts, it was usually found that the dominant chain termination pathway under sufficient monomer concentration is β-hydrogen transfer to the monomer (BHT). In the present case, we have already shown for the small "model" system that the BHT barrier is rather large. We will now see how this is modified by steric bulk.

The direct precursor for BHT is the π-complex (**3a**), in which the alkyl chain forms a β-agostic bond with the metal center. However, steric pressure elevates this particular π-complex above the dissociation asymptote, so that it is far less stable than all other π-complexes in this system. Once this π-complex is formed (at a considerable expenditure of 56 kJ/mol relative to **3b**), the actual BHT process, consisting of an elongation of the β-agostic bond, only consumes an additional 18 kJ/mol. Thus, with a total activation barrier of 74 kJ/mol (relative to **3b**), it is highly unlikely that BHT is the dominant chain termination process for this catalyst.

To successfully complete a chain transfer/termination by BHT, the vinyl-terminated chain has to be ejected. The ejection of the chain has a barrier on the PES, with the transition state **6** → **7** lying 46 ± 10 kJ/mol above the dissociation asymptote. Note that the fact that there is a barrier for this process again is related to the steric bulk around the active site. The ethyl ejection product is 3 kJ/mol more stable than the propyl product. Thus, ethene− and propene−metal bond strengths in this system are approximately equal.

Chain Termination by BHE. The competing chain termination step (except for counterion-induced chain termination) is β-hydrogen elimination (BHE). For d^0 and d^8 systems, this is usually less feasible than BHT. However, under special circumstances that can be induced sterically, BHE can take over from BHT.

In the present case, the BHE transition state **2b** → **5** lies 52 kJ/mol above **2a** and the separated olefin and 24 kJ/mol above **2b** and the separated olefin. The question of which termination mechanism is dominant is therefore dependent upon monomer partial pressure and, also, upon the free energy barrier to olefin capture. We have previously shown that the free energy contribution to the capture barrier is far from negligible and can induce capture barriers on the order of 50 kJ/mol, even in cases where there is no barrier on the PES. Since in the present case there is a potential energy barrier to capture, it might be conjectured that the entropic contribution to the capture barrier will be decisive in determining the capture rate and, thus, will determine the relative rates of BHE (first order) vs BHT (second order). In the absence of reliable free energy data (see also discussion), we cannot give preference to any given termination mechanism based on kinetic barriers on the PES at this point.

It seems, however, that the completing step of BHE, namely the dissociation of the vinyl-terminated chain, tips the scales in favor of the BHT mechanism. The dissociated BHE product lies 183 kJ/mol above **2a**, which seems an unsurmountable barrier to the completion of BHE. Aiding the dissociation process by an incoming monomer seems an unfeasible proposal, since the steric crowding around the active site is too strong to allow entrance of another monomer. *We therefore draw the preliminary (in the absence of detailed free energy data) conclusion that BHT is (besides counterion-induced termination) the dominant chain termination step in the present system. However, our data leads us to the conclusion that neither BHT ($\Delta E^{\ddagger} = 76$ kJ/mol) nor BHE (thermodynamic ejection barrier 183 kJ/mol) can account for the experimentally observed modest molecular weights (14 000−26 000) when compared to the insertion barrier ($\Delta E^{\ddagger} = 26$ kJ/mol). We thus expect chain transfer to the counteranion to give rise to the experimentally observed lower molecular weights.*

Chain Isomerization after BHT. A possible alternative outcome of a BHT event is chain isomerization. This can happen if the barrier for rotation of the vinyl-terminated chain is actually lower than the barrier for its ejection. We have studied the rotation of the vinyl-terminated chain and found that the barrier for this process **6a** → **6b** is very high and involves partial dissociation of the ancillary nitrogen ligands. Thus, with the rotational barrier being higher than the barrier for ejection, isomerization after is not feasible for this catalyst.

Chain Isomerization after BHE. Brookhart's Ni and Pd systems are able to create a highly branched polymer by a mechanism that is a combination of BHE and chain rotation. This does not seem to be a feasible route for the present catalyst. The chain isomerization barrier (by rotation of the vinyl-terminated chain after BHE; **5a** → **5b**) is 51 kJ/mol, with the transition state 95 kJ/mol above **2a** (Figure 1). Rotation of the chain involves partial dissociation of the vinyl terminus from the Co center, so that any attempt at isomerization would most likely result in displacement of the chain by a solvent molecule. *We conclude that neither the post-BHE nor the post-BHT isomerization pathway is feasible for the present catalyst. This is mostly an effect of steric congestion around the active site, which prohibits rotations of the chain.*

Concluding Remarks

We have investigated the mechanisms and energetics of ethylene polymerization by the catalyst [2,6-bis((1-(2,6-isopropylphenyl)imino)ethyl)pyridine]cobalt(II) catalyst. Comparison with its "generic" counterpart, [2,6-bis(iminomethyl)pyridine]cobalt(II), allows us to show how the potential surface generated by the metal and its immediate surroundings is modified by additional steric bulk attached to the ancillary ligand.

Downloaded by CARLI CONSORTIUM on June 30, 2009
Published on December 1, 1999 on http://pubs.acs.org | doi: 10.1021/om990392m

We find that the doublet and quartet potential energy surfaces are relatively close to each other for this catalyst. By comparing results for several density functionals, we predict that the doublet is the most stable electronic state for all cationic species (except for the alkyl precursors **2**, for which the quartet is slightly more stable) and that the halide precursor has a quartet electronic ground state, due to its weak ligand field.

The "model" system [2,6-bis(iminomethyl)pyridine]-cobalt(II) is, according to our calculations, an ethylene polymerization catalyst, producing a low-molecular-weight polymer. The insertion barrier relative to the most stable π-complex is 40 kJ/mol, compared to a BHT barrier of 50 kJ/mol. Under low monomer partial pressure we predict the "model" system to perform poorly: the barrier for BHE is only 28 kJ/mol.

Attachment of steric bulk results in dramatic changes to catalytic behavior, as follows.

(a) We observe that olefin uptake is no longer barrierless on the PES but indeed has substantial barriers between 20 and 40 kJ/mol, depending on the entrance channel. It is, however, strictly necessary to exert caution when interpreting these results. Our capture barriers relate to a 0 K picture and, hence, do not account for effects of finite temperature. We estimate, on the basis of previous experience, that the actual capture barriers are substantially higher. Olefin capture is also less exothermic than for the "model" system. Without further modifications of the ancillary ligand, we predict this catalyst to be rather inefficient for polymerizing monomers larger than ethylene. This is a logical consequence of the fact that the narrow entrance channel acts selectively toward small monomers.

(b) Steric bulk imposes additional corrugation upon the PES, so that there are more metastable conformations for one and the same compound. Furthermore, this corrugation makes conversion between different conformers more difficult, as seen for example in the rearrangement **3d** → **3b**.

(c) As already observed for the Ni and Pd systems developed by Brookhart's group, we see here that the steric pressure serves to lower the olefin insertion barrier, while increasing the termination barriers. This is because steric bulk favors compressed transition states such as insertion over extended transition states such as BHT or BHE.

(d) Chain propagation can proceed over three different transition states (FS, **3b** → **4a**; BS, **3c** → **4b**; apical FS, **3d** → **4a**). However, the FS TS is by far the energetically lowest one and is projected as the focus of the two main propagation channels (the FS and BS-FS propagation channels, respectively).

(e) A further effect of steric bulk is that isomerization pathways are completely suppressed. Isomerization by rotation of a vinyl-terminated chain is possible with the Ni and Pd diimine relatives of the present systems, but the additional steric crowding due to having a tridentate instead of a bidentate ancillary ligand makes this impossible. Isomerizations both after BHT and after BHE have been investigated and found energetically unfeasible.

(f) Although we were able to obtain a picture of the PES of the catalytic cycle, we cannot unambiguously state which termination pathway(s) dominate under experimental conditions. A more detailed understanding will necessitate simulations that take into account entropic factors and also counteranion-induced chain termination.

We have shown that purely steric modifications can drastically alter the performance of the present system. Above all, it seems desirable to facilitate olefin capture by creating additional openings onto the active site without compromising the insertion activity.

The corresponding iron(II) systems have been analyzed elsewhere.[4c] We find the generic [2,6-bis(iminomethyl)pyridine]iron(II) complex to bind too strongly to ethylene for any further chemical transformation to take place. The steric bulk introduced by R = 2,6-C_6H_4(i-Pr)$_2$ in the "real" [2,6-bis(1-((2,6-isopropylphenyl)imino)ethyl)-pyridine]iron(II) system was found to weaken the olefin bond and lower the barrier of insertion.

Acknowledgment. This investigation has been supported by the National Sciences and Engineering Research Council of Canada (NSERC) and by the donors of the Petroleum Research Fund, administered by the American Chemical Society, as well as by Novacor Research and Technology Corp. (NRTC) of Calgary.

Supporting Information Available: Cartesian coordinates and total energies of all species mentioned in the text and a full listing of the molecular mechanics force field parameters utilized. This material is available free of charge via the Internet at http://pubs.acs.org.

OM990392M

Downloaded by CARLI CONSORTIUM on June 30, 2009
Published on December 1, 1999 on http://pubs.acs.org | doi: 10.1021/om990392m